Fundamental Journals
International Journal of Fundamental Physical Sciences (IJFPS) ISSN:2231-8186
IJFPS, Vol 4, No 2, pp 43- 54, June , 2014 S.N. Hosseinimotlagh
DOI:10.14331/ijfps.2014.330065
http://dx.doi.org/10.14331/ijfps.2014.330065

Scrutiny on the Static Behavior of Physical Parameters for ITER90H-P Fusion Reactor Using Deuterium–Tritium and Deuterium-Helium Mixtures

S.N. Hosseinimotlagh[1, 2*], S.Kianafraz [2], H.Arshadi [2], N.Jamshidi [2]

[1]Department of Physics, Islamic Azad University, Shiraz Branch, Shiraz, Iran
[2]Department of Physics, Islamic Azad University, Arsenjan Branch, Fars, Iran

Email: hoseinimotlagh@ hotmail.com

(*Received Feb 2014; Published June 2014*)

ABSTRACT

In this work, the performance of fusion reactor ITER90H-P with considering D–T and *D-*^{3}*He* fuels are examined by writing the dynamics equations on the system reactor. Therefore, we solve these equations analytically in the steady state. In this state we determine the optimum conditions for achieving the maximum fusion gain .In addition, we ignore the impurities because we need to high performance points without impurities. Our calculations in this paper show that we have maximum fusion gain for DT and *D-*^{3}*He* fusion reactions in steady state at resonance temperature Kev70 for D-T fusion reaction respectively .Their maximum values of fusion gain are equal to 6.01 for D-T fuel-andthe0.012 for *D-*^{3}*He*, respectively. Therefore, currently, using *D-*^{3}*He* as a fusion fuel is not recommended.

Keywords: Steady, Fusion Gain, Power, Helium, Tritium

DOI:10.14331/ijfps.2014.330065

INTRODUCTION

The objective of international thermonuclear experimental reactor (ITER) is to demonstrate the sciatic and technological feasibility of applying fusion energy for peaceful purposes. ITER will be able to produce a 'burning' D-T plasma for the first time, where the majority of the plasma heating is self-produced from fusion-generated alpha particles. It employs three primary operation modes for demonstrating controlled burning plasmas; the reference mode, the steady-state mode and the hybrid operation mode. The reference operation mode, the ELMy H-mode, is expected to achieve extended burn in an inductively-driven D-T plasma with a fusion power of 500 MW and a high fusion gain $Q \sim 10$ (the ratio of fusion power to the external heating power) for a burn duration of 300-500 s. The steady-state operation mode aims at demonstrating steady-state operation using a non-inductive current drive with $Q > 5$ lasting for ~3000 s. In steady-state plasmas, a large fraction (>50 %) of the plasma current will be driven by the self-generated bootstrap current originating from the pressure gradient of the plasma. The hybrid operation mode combines inductive and non-inductive current drives at a plasma current lower than the inductive reference operation mode. The hybrid mode is expected to produce high fusion power and long pulses (>1000 s) so that engineering tests of reactor-relevant components, such as breeding blankets, are going to be fulfilled. The construction and operation of ITER is the next step towards controlled nuclear fusion. The main goal of the ITER project is to demonstrate that power generation by nuclear fusion is feasible in an economically and environmentally acceptable way. In a fusion reactor the hot plasma is confined by the magnetic fields generated by the superconducting coils system and the plasma current. Thus, the superconducting magnet system is an indispensable component. The superconducting magnet system is designed with the low temperature superconductors and needs to operate at liquid helium temperature (~4.5K). In order to charge the superconducting magnet system (at 4.5 K) from the power supply at room temperature, a current feeder system is required. It consists of a superconducting feeder, a current lead and a water-cooled Aluminum bus bar. So, the current feeder system basically acts as current transmission line from 4.5K to 300K. In the present design, the ITER magnet system uses Nb3Sn for the Toroidal Field and Central Solenoid coils and NbTi for the Poloidal Field (PF) and Correction Coil magnets respectively. For practical reasons the superconductor feeder will also be made of NbTi. The superconducting current feeder system requires higher stability and safety margin than the magnets because in any kind of operation or fault condition, the large amount of magnetic stored energy in the coils must be extracted safely via the current feeder paths. Fig1 shows a sketch of the current feeder system for ITER using a current lead and a water-cooled Aluminum bus bar.

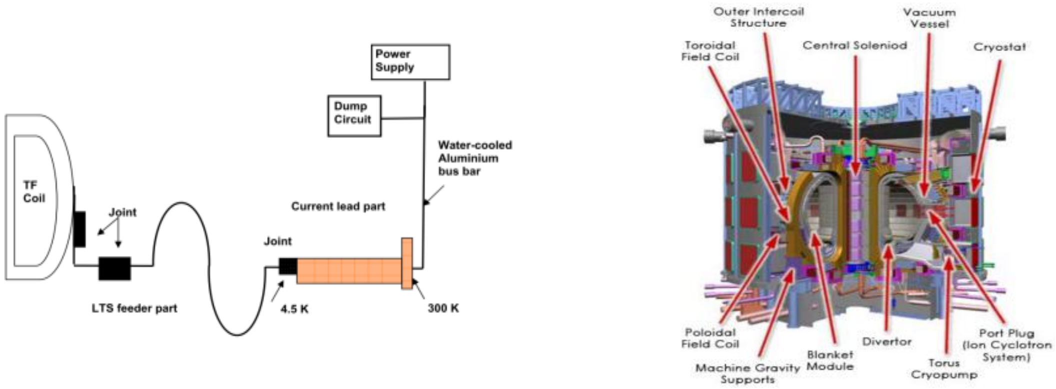

Fig1. (a) Schematic layout of the present design of current feeder system for ITER.(Kadomtsev, 1992; Pinna & Rizzello, 2002; Wesson, 2011) **(b)** The ITER-FEAT device and major components

With these improvements, it is hoped that ITER will also allow for the possibility of reaching a more important goal, one that will be essential for a fusion power plant. For a deuterium-tritium plasma, once heating of alpha particles (the Helium nuclei product of fusion), not by external input but by the fusion process itself, is equal to the heat loss through the vessel walls and diverter, the plasma becomes self-sustaining and is said to be ignited, or burning. External heating can be turned off, and the plasma will continue to exist and induce fusion.

Table1. ITER machine parameters (Schuster, Krstic, & Tynan, 2003; Uckan, 1993; Uckan et al., 1994).

Parameter	Value
Major/minor radius	8.14 m/2.80 m
Plasma configuration	Single null diverter
Plasma Vertical elongation/triangularity (at 95% poloidal flux)	1.6/0.24
Plasma volume	~2000 m^3
Plasma surface area	~1200 m^2
Nominal plasma current	21 MA
Electron Density	$0.98 \cdot 10^{20}$ m^{-3}
Volume Average Temperature	12.9 keV
Toroidal field	5.68 T (at R = 8.14 m)
MHD safety factor (q95)	~3.0 (at 21 MA)
Volume average β / β N	0.030 / 2.29
Fusion power (ignited, nominal)	1.5 GW
Plasma thermal energy content	1.07 GJ
Plasma magnetic energy content	1.1 GJ
Confinement Mode	ELMy H-mode
Radiation from plasma core	118 MW
Transport Power Loss	182 MW
Transport Energy Confinement time τ_E	5.9 sec
Z_{eff} - effective ion charge	1.9
Average neutron wall loading	~1 MW/m^2 (at 1.5 GW)
Lifetime neutron flounce	$\geq$ 1 MWa/m^2
Burn duration (ignited, inductive current drive)	$\geq$ 1000 s
Available auxiliary heating power	100-150 MW
In-vessel tritium inventory safety limit	1 kg

With no heating (energy input), the Q factor ratio tends to infinity and the fusion process is controlled in steady state only by the fuelling rate to the torus. In Table 1 the ITER machine parameters are given.

In order to nuclear fusion reactor is economically affordable, the system must stay for a long time in the burning plasma steady state with performance points at high Q .Here Q is the ratio of auxiliary power to fusion power which is called fusion. Thus, in this paper, under these conditions we will have study on the behavior of ITER 90 HP fusion reactor in the steady-state for two fusion fuel such as D-T and *D-^{3}He* with taking into account the system temperature variations. Finally, we determine the required conditions to achieve high fusion gain.

The rest of the paper is organized as follows in section 2, Reactivity parameter for D–T and *D-^{3}He* fusion reactions is presented. In section 3, Nonlinear point Kinetic equations governing on the ITER 90 HP fusion reactor ITER 90 HP for the D-T and *D-^{3}He* fuel are stated, and these equations are solved analytically.

Section 4 is concerned with these equations are solved analytically. Section 5 discusses the results of the Calculation and comparison of required parameters for study ofITER90H-p fusion reactor at steady state for both fuel D-T and *D-^{3}He*. Finally, section 6 contains some conclusions concerning this work and further extensions and research suggested in this direction.

REACTIVITY PARAMETER FOR D–TAND *D-^{3}HE* FUSION REACTIONS

This paper, presents a strategy for the development of *D-^{3}He* fusion for terrestrial and space power .the approach relies on modest plasma confinement progress in alternate fusion concepts and on the relatively less challenging engineering, environmental and safety features of a *D-^{3}He* fueled fusion reactor compared to a D-T fueled fusion reactor. The *D-^{3}He* benefits include full-lifetime materials, reduced radiation damage, less activation, absence of tritium breeding blankets, highly efficient direct energy conversion, easier maintenance and proliferation resistance. The main fusion fuels are,

$$D + T \rightarrow {}^4He + n + 17.6\ MeV$$
$$D + {}^3He \rightarrow {}^4He + p + 18.4\ MeV$$

Also another important parameter is reactivity of D–T and *D-^{3}He* which depends on the temperature. **a)** Bucky Reactivity is temperature dependent T (keV) and is given by,

$$<\sigma v>_{DT} = exp\left(\frac{a_1}{T^r} + a_2 + a_3 T + a_4 T^2 + a_5 T^3 + a_6 T^4\right) \quad (1)$$

Here $\boldsymbol{a_i}$ and r are given in the Table 2.

Table 2. Numerical values of $\boldsymbol{a_i}$and r parameters for D-T and *D-^{3}He* fusion reactions using Bucky formula (Hively, 1977)

	D^3He	DT
a_1	2.1377692×10^1	2.7764468×10^1
a_2	2.5204050×10^1	3.1023898×10^1
a_3	7.1013427×10^{-2}	2.7889999×10^{-2}
a_4	1.937545×10^{-4}	5.5321633×10^{-4}
a_5	4.9246592×10^{-6}	3.0293927×10^{-6}
a_6	3.9836572×10^{-8}	2.5233325×10^{-8}
r	0.2935	0.3597

b) Bosch and Hale (1992) activity is given by the following formula

$$<\sigma v> = C_1 \theta e^{-3\xi}\sqrt{\frac{\xi}{(m_r c^2 T^3)}} \quad (2)$$

ξ، θ and B_G are

$$\xi = \left(\frac{B_G^2}{4\theta}\right)^{\frac{1}{3}} \quad (3)$$

$$\theta = T\left(1 - \frac{T(C_2 + T(C_4 + T C_6))}{1 + T(C_3 + T(C_5 + T C_7))}\right)^{-1} \quad (4)$$

$$B_G = \pi\alpha Z_1 Z_2\sqrt{2m_r c^2} \quad (5)$$

The constants values of C_1 to C_7 in these equations for different fusion reactions are given in Table(3)

Table 3. The constants values of $C_1$to $C_7$for different fusion reactions (Bosch,et al. 1992)

	$^3He(d,p)\ ^4He$	$D(d,p)T$	$D(d,n)\ ^3He$	$T(d,n)\ ^4He$
C_1	1.17E-09	5.43E-12	5.66E-12	5.51E-10
C_2	1.51E-02	5.86E-03	3.41E-03	6.42E-03
C_3	7.52E-02	7.68E-03	1.99E-03	-2.03E-03
C_4	4.61E-03	0.00E+00	0.00E+00	-1.91E-05
C_5	1.35E-02	-2.96E-06	1.05E-05	1.36E-04
C_6	-1.07E-04	0.00E+00	0.00E+00	0.00E+00
C_7	1.37E-05	0.00E+00	0.00E+00	0.00E+00
$m_r c^2 (keV)$	1124656	937814	937814	1124572

According to the above equations and the data in Tables (2) and (3) we plotted the $<\sigma v>$ versus temperature for the fusion reaction of D-T and *D-^{3}He* for both of Bucky and Bosch-Hale formula (Bosch & Hale, 1992).

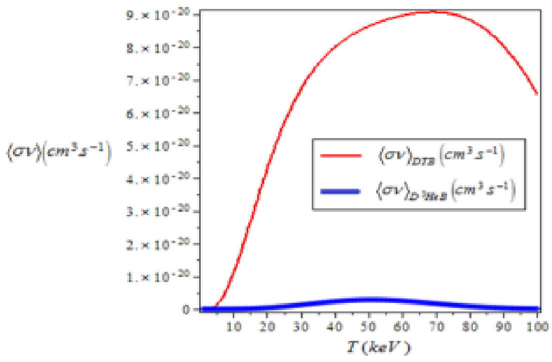

a

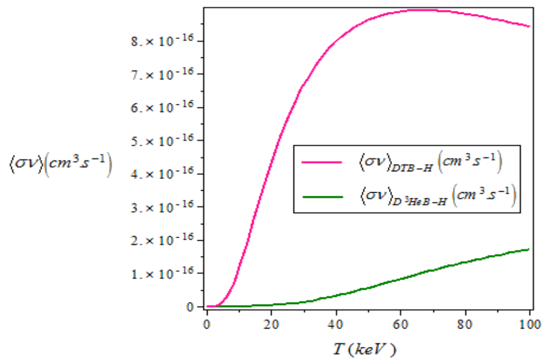

b

Figure 2. Comparison of the graphs of fusion reactions reactivity variations for **(a)** D-T **(b)** *D-^{3}He* Versus temperature by the two methods, Bucky and Bosch-Hale.

As shown in Figure2-a , the reactivity of D – T fusion reaction is greater than $D-{}^3He$ .Because $<\sigma v>_{\mathrm{DT}}$ at 70 kev temperature has a maximum value thus 70 kev is temperature resonance.the value of D – T reactivity at this temperature approximately 10 times is greater than $D-{}^3He$.By viewing the obtained numerical values and Figure2-bwe find that the difference between the two ways of calculating reactivity is minimal and since that the method of Bucky is newer than Bosch-Hale (Bosch & Hale, 1992)in our calculations we use this.

NONLINEAR KINETIC EQUATIONS

Nonlinear point Kinetic equations, governing on the ITER 90 HP fusion reactors ITER 90 HP for the D-T and $D-{}^3He$ fuel. In this work, we have used fusion reactor in which approximately particle energy balance equations for two D-T and $D-{}^3He$fuel are given by, **(a)** Nonlinear point Kinetic equations governing on the D-T fuel.

$$\frac{dn_\alpha}{dt}=\frac{-n_\alpha}{\tau_\alpha}+\left(\frac{n_{DT}}{2}\right)^2<\sigma v>_{\mathrm{DT}} \quad (6)$$

$$\frac{dn_{DT}}{dt}=\frac{-n_{DT}}{\tau_{DT}}-2\left(\frac{n_{DT}}{2}\right)^2<\sigma v>_{\mathrm{DT}}+\frac{n_n}{\tau_d} \quad (7)$$

$$\frac{dn_n}{dt}=\frac{-n_n}{\tau_d}+S \quad (8)$$

$$\frac{dn_I}{dt}=\frac{-n_I}{\tau_I}+S_I \quad (9)$$

$$\frac{dE}{dt}=\frac{-E}{\tau_E}+P_\alpha+P_{Ohmic}-P_{rad}+P_{aux} \quad (10)$$

(b) Nonlinear point Kinetic equations governing on the $D-{}^3He$fuel

$$\frac{dn_\alpha}{dt}=\frac{-n_\alpha}{\tau_\alpha}+\left(\frac{n_{D\,{}^3He}}{2}\right)^2<\sigma v>_{D\,{}^3He} \quad (11)$$

$$\frac{dn_{D\,{}^3He}}{dt}=\frac{-n_{D\,{}^3He}}{\tau_{D\,{}^3He}}-2\left(\frac{n_{D\,{}^3He}}{2}\right)^2<\sigma v>_{D\,{}^3He}+\frac{n_n}{\tau_d} \quad (12)$$

$$\frac{dn_n}{dt}=\frac{-n_n}{\tau_d}+S \quad (13)$$

$$\frac{dn_I}{dt}=\frac{-n_I}{\tau_I}+S_I \quad (14)$$

$$\frac{dE}{dt}=\frac{-E}{\tau_E}+P_\alpha+P_{Ohmic}-P_{rad}+P_{aux} \quad (15)$$

In these equations,n_I و n_n, $\boldsymbol{n}_{D\,{}^3He}$, n_{DT}, n_α are the alpha particle, deuterium-tritium, deuterium-helium3, and the neutral fuel (defined as the number of fuel atoms divided by the core volume) and impurity densities, respectively .$\boldsymbol{\tau_\alpha}$ is the confinement time for the alpha particles, S is the refueling rate, τ_{DT}, $\boldsymbol{\tau}_{D\,{}^3He}$ are the confinement time for ionized fuel particles of D, T and ${}^3He$, D respectively.τ_d is the controller lag time ,E is the plasma energy,τ_E is the energy confinement time,τ_I is the confinement time for the impurities, $S_I$is the impurity injection rate, $Q_\propto$= 3.52MeV is the energy of the alpha particles. $\boldsymbol{P_\alpha}$, P_{aux} , $\boldsymbol{P_{rad}}$, $\boldsymbol{P_{Ohmic}}\boldsymbol{P_i}$ and $\boldsymbol{P_f}$are the alpha power, auxiliary power , radiation loss ,Ohmic power, the net plasma heating power and fusion power ,respectively that are given for both of fuels D – T and $D-{}^3He$ (Eremin & Shishkin, 2008)

$$P_{\alpha DT}=\left(\frac{n_{DT}}{2}\right)^2<\sigma v>_{\mathrm{DT}}Q_{\alpha DT} \quad (16)$$

$$P_{\alpha D\,{}^3He}=\left(\frac{n_{D\,{}^3He}}{2}\right)^2<\sigma v>_{D\,{}^3He}Q_{\alpha D\,{}^3He} \quad (17)$$

$$P_{auxDT}=\frac{E}{\tau_E}-\left(\frac{n_{DT}}{2}\right)^2<\sigma v>_{\mathrm{DT}}Q_{\alpha DT}-P_{Ohmic}+A_{bDT}(n_{DT}+2n_\alpha)(n_{DT}+4n_\alpha)\sqrt{\frac{2E_{DT}}{3N_{DT}}} \quad (18)$$

$$P_{auxD\,{}^3He}=\frac{E}{\tau_E}-\left(\frac{n_{D\,{}^3He}}{2}\right)^2<\sigma v>_{D\,{}^3He}Q_{\alpha D\,{}^3He}-P_{Ohmic}+A_{bDT}\left(n_{D\,{}^3He}+2n_\alpha\right)\left(n_{D\,{}^3He}+4n_\alpha\right)\sqrt{\frac{2E_{D\,{}^3He}}{3N_{D\,{}^3He}}} \quad (19)$$

E_i,N_i, are the total energy and density for ($i=DT, D\,{}^3He$),

$$E_{DT}=\frac{3}{2}N_{DT}T \quad (20)$$

$$E_{D\,{}^3He}=\frac{3}{2}N_{D\,{}^3He}T \quad (21)$$

and

$$N_{DT} = 2n_{DT} + 3n_{\alpha DT} + (Z_I + 1)n_I \qquad (22)$$

$$N_{D\ ^3He} = 2n_{D\ ^3He} + 3n_{\alpha D\ ^3He} + (Z_I + 1)n_I \qquad (23)$$

$$P_{radDT} = A_{DT} \times Z_{effDT}\, n_e^2 \sqrt{T} \qquad (24)$$

$$P_{radD\ ^3He} = A_{D\ ^3He} \times Z_{effD\ ^3He}\, n_e^2 \sqrt{T} \qquad (25)$$

Where

$$A_{DT} = 4.85 \times 10^{-37} \left(\frac{Wm^3}{\sqrt{keV}}\right) \qquad (26)$$

$$A_{D\ ^3He} = 5.35 \times 10^{-37} \left(\frac{Wm^3}{\sqrt{keV}}\right) \qquad (27)$$

The effective charge ($Z_{eff\,i}$) and electron density (n_{ei}) for D – T and $D - {}^3He$ are,

$$Z_{effDT} = \frac{n_{DT} + 4n_{\alpha DT}}{n_{DT} + 2n_{\alpha DT}} \qquad (28)$$

$$Z_{effDT} = \frac{n_{D\ ^3He} + 4n_{\alpha D\ ^3He}}{n_{D\ ^3He} + 2n_{\alpha D\ ^3He}} \qquad (29)$$

$$n_{eDT} = n_{DT} + 2n_{\alpha DT} + Z_I n_I \qquad (30)$$

$$n_{eD\ ^3He} = n_{D\ ^3He} + 2n_{\alpha D\ ^3He} + Z_I n_I \qquad (31)$$

Z_I is the atomic number of impurities.

$$P_{OhmicDT} = \eta_{DT}\, j^2 \qquad (32)$$

$$P_{OhmicD\ ^3He} = \eta_{D\ ^3He}\, j^2 \qquad (33)$$

Here j is the plasma current density and n is electron density such that $5 \times 10^5 \leq j(mA) \leq 1.5 \times 10^6$ and $0 \leq n_e(m^{-3}) \leq 14 \times 10^{19}$ and η is the Spitzer resistivity in which for D – T and $D - {}^3He$ we have (Spitzer Jr, 1965; Spitzer, 2013; Trintchouk, Yamada, Ji, Kulsrud, & Carter, 2003).

$$\eta_{DT} =$$

$$1.03 \times 10^{-4} \times T^{\frac{-3}{2}} \times Z_{effDT} \times \ln\left(\frac{T^{\frac{3}{2}}}{\sqrt{n} \times e^3 \times Z_{effDT} \times \sqrt{3.14}}\right) \qquad (34)$$

$$\eta_{D\ ^3He} =$$

$$1.03 \times 10^{-4} \times T^{\frac{-3}{2}} \times Z_{effD\ ^3He} \times \ln\left(\frac{T^{\frac{3}{2}}}{\sqrt{n} \times e^3 \times Z_{effD\ ^3He} \times \sqrt{3.14}}\right) \qquad (35)$$

Here T and e are the electron temperature and charge such that, $e = 1.6 \times 10^{-19} c$

$$P_i = P_{\alpha_i} - P_{rad_i} + P_{aux_i} + P_{Ohmic_i} \qquad (36)$$

Where i=DT, D3He and

$$P_{fuDT} = \left(\frac{n_{DT}}{2}\right)^2 < \sigma v >_{DT} Q_{DT} \qquad (37)$$

$$P_{fuD\ ^3He} = \left(\frac{n_{D\ ^3He}}{2}\right)^2 < \sigma v >_{D\ ^3He} Q_{D\ ^3He} \qquad (38)$$

Also, the gain (Q) of this type of reactor for the D–T and $D - {}^3He$ reactions D –T are given in the following,

$$Q_{DT}^{-} = \frac{P_{fuDT}^{-}}{P_{auxDT}^{-}} \qquad (39)$$

$$Q_{D\ ^3He}^{-} = \frac{P_{fuD\ ^3He}^{-}}{P_{auxD\ ^3He}^{-}} \qquad (40)$$

Also from the plotting of equations (32) to (35) we have two-dimensional and three-dimensional graphs of resistivity and Ohmic power variations for ITER 90 HP fusion reactor in terms of electron density and temperature for D – T and $D - {}^3He$ in the temperature interval 0-100 (kev). (see Figures (3) and (4)).

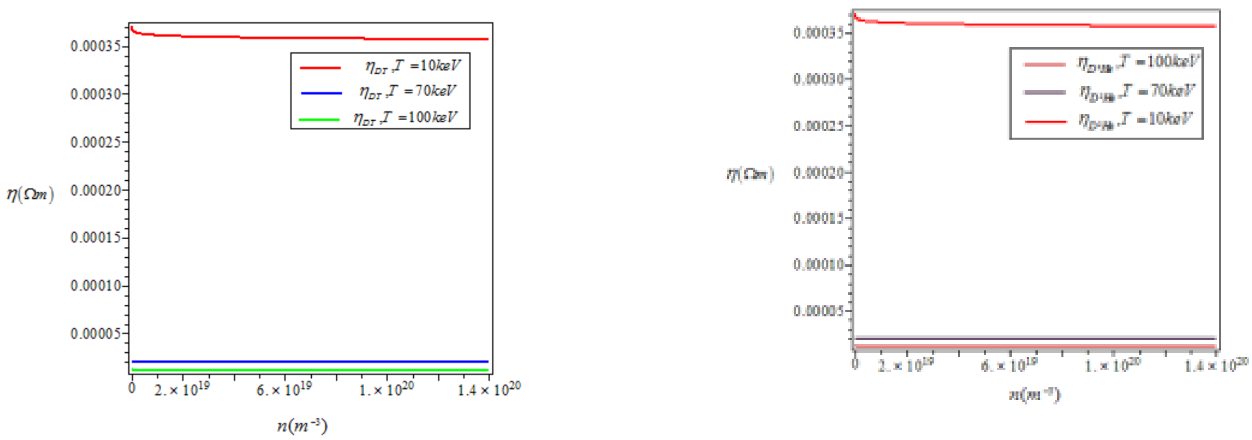

a **b**

Fig3. Comparison of two-dimensional resistivity curves of two fuels **(a)** D - T b) $D - {}^3He$ at three temperatures T = 10 *keV*, T = 70 *keV* and T = 100 *keV* in terms of electron density variations.

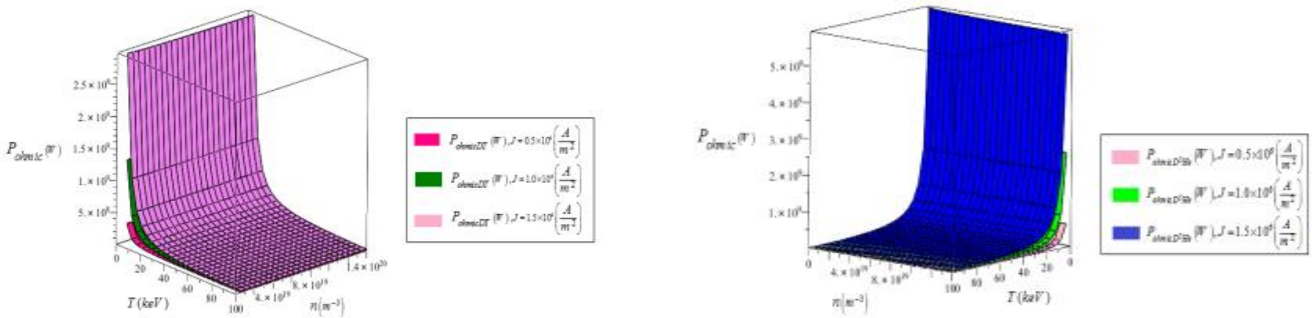

a b

Fig4. Comparison of three-dimensional diagrams of the Ohmic power for two fuel **(a)** D-T **(b)** $D-{}^{3}He$ at three different current density, $j=0.5\times10^{6}(A/m^{2})$, $j=1\times10^{6}(A/m^{2})$ and $j=1.5\times10^{6}(A/m^{2})$ in terms of the electron density variations and temperature.

From viewing of two-and three-dimensional graphs of resistivity and Ohmic power for both D - T and $D-{}^{3}He$ fuel we find that both resistivity (η) and Ohmic power ($\boldsymbol{P_{Ohmic}}$) decrease by increasing of electron density at each temperature but increase by decreasing temperature. Energy confine meantime of the reactor ITER90H-P is given by (Uckan, 1993).

$$\tau_E = f\ 0.082\ I^{1.02}R^{1.6}B^{0.15}A_i^{0.5}\ k_X^{-0.19}p^{-0.47} \qquad (41)$$

Where the isotopic number for (50:50) D-T mixture percentage is 2.5. The factor scale f depends on the confinement situation I, R, Band Pare plasma current, plasma radius, toroidial plasma field and net plasma heating respectively, in which and its numerical values are given in Table(4) .

Table(4). Numerical values of ITER90H-P fusion reactor (Schuster.,et al.2003)

f	$I(mA)$	$R(m)$	$B(Ts)$	A_i	k_X	$P(MW)$
0.425	22	6	4.85	2.5	1.98	75

Confinement times in terms of different values are scaled with energy confinement time τ_E as $\tau_d = k_d\tau_E$, $\tau_\alpha = k_\alpha\tau_E$, $\tau_{DT} = k_{DT}\tau_E$ and $\tau_{D\,^3He} = k_{D\,^3He}\tau_E$. In addition, in our calculations we ignore of impurities because we interested to free conditions of impurities.

Calculation of required parameters for study of ITER90 H-p fusion reactor at steady state for $D-T$ and $D-{}^{3}He$

Note that, the values of variables in which obtaining the steady-state for fusion reactor ITER90H-pare shown with a line above them. So, the numerical values of these variables$\bar{n_I}$, $\bar{n_n}$, $\bar{n_{D\,^3He}}$, $\bar{n_{DT}}$, $\bar{n_\alpha}$ and energy state variable $\bar{E}$ at refueling $\bar{S}$ and auxiliary power $\bar{P_{aux}}$ at steady state from solving of nonlinear point kinetic equations can be calculate with the inserting left side non-linear equations (6) to (15) equal to zero. Our obtained figures are given in the following for both D-T and $D-{}^{3}He$ fuel at steady-state in temperature range0 to100kev. It should be noted that the two parameters k_d and $k_\alpha$used indrawingthegraphsareconsidered constantand its numerical values are $k_d=3$ and $k_\alpha=7$.

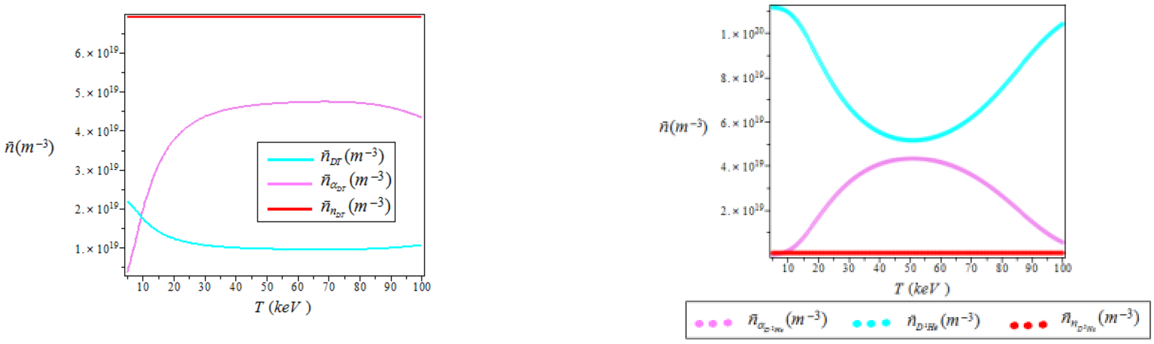

a b

Figure5. Comparison of variations of neutral fuel density, **(a)** deuterium and tritium and alpha particles of D-T. **(b)** deuterium and Helium and alpha particles of $D-{}^{3}He$ in the steady state at temperature range of 0-100 *Kev*.

From Fig.5 we see that particle density of D and T is declining because due to nuclear fusion of D-T, D and T particles are consumed and its amount are decreased. Then system goes toward relative equilibrium and the value of densities could be a fixed amount. Density of the alpha particles is increasing because due to D-T fusion reaction alpha particles are produced thus the value of them amount increases. Then since that they may have escaped from system thus the value of them are reduced and then since the system goes to ward to a relative equilibrium the numerical values of densities could be a fixed amount. Neutral particle density of the fuel is injected at a constant rate$7 \times 10^{19}(m^{-3})$ at all temperatures. Also, for the $D-{}^3He$ reaction in temperature range of 0 to100kev, we see that alpha particle density, at first is increasing because as shown in Fig (2) to a temperature of 60 (keV), $<\sigma v>_{D\ {}^3He}$ and therefore number of fusion reactions increase. As the temperature increases $<\sigma v>_{D-3He}$ and thus number of fusion reactions decrease. Therefore alpha particle density is decreased. Initially the particle density of D and ${}^3He$ decrease because according of Fig (2) till temperature 70 (keV), $<\sigma v>_{D\ {}^3He}$ and thus number of fusion reactions increase therefore more fuel is consumed. Therefore, the particle density of D and ${}^3He$ is reduced whose its decreasing processes in this temperature range is perfectly obvious. Then in the temperature range70 to100 (keV),$<\sigma v>_{D\ {}^3He}$ and thus number of fusion reactions of $D-{}^3He$ are reduced. Therefore low $D-{}^3He$ fuel is consumed, therefore gradually is increased. Neutral particle density of the fuel is injected at a constant r at eatal l temperatures. Since that the magnitude of neutral density versus temperature is order of $6.98 \times 10^{17}(m^{-3})$ therefore in comparison with thealpha particle ,D, and T densities$(10^{19}(m^{-3}))$ is very low, that can be seen in the Figure(5).Also Figure (6) shows variations of energy density in terms of temperature for both fuel D-T and $D-{}^3He$ at steady state.

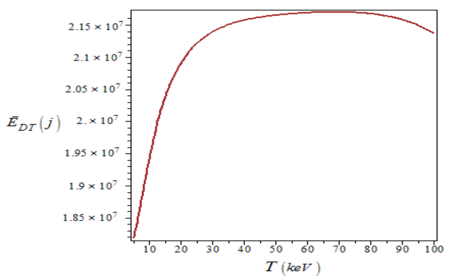

a

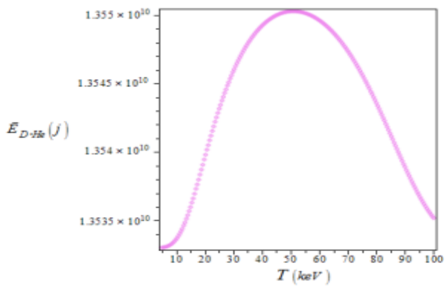

b

Fig6. Energy density variations of **(a)** D-T and **(b)** $D-{}^3He$ c) comparison of D-T and $D-{}^3He$ in the steady-state at the temperature range0 to100 Kev.

From Fig 6 for D-T and $D-{}^3He$ fuels we observe that initially the energy density of these fuel increases with increasing temperature until the temperature reaches the resonance and then gradually reduced. Its reason is that with increasing temperature number of fusion increases and thus more energy is produced such that in 70 *KeV* which known as resonance temperature of D-T fusion reaction we have maximum energy. With increasing temperature, $<\sigma v>_{\mathrm{DT}}$ is reduced. Therefore, the numbers of fusion reactions are reduced and thus energy is decreased. The same trend can be seen for the $D-{}^3He$ reaction except that since $50keV$ is the resonance temperature of $D-{}^3He$. Therefore, at the resonance temperature of $D-{}^3He$ fusion reaction we will have the maximum energy. With having the values of $n^-_{nDT}, n^-_{\alpha DT}, n^-_{n_D\ {}^3He}, n^-_{\alpha_D\ {}^3He}, n^-_{D\ {}^3He}, n^-_{DT}$ and ignoring of impurities and using equations (18) to (25) , (28), (29) and (36) to (40) respectively, quantities of auxiliary power (P^-_{aux}), total energy density (E^-), total density (N^-), radiative power loss (P^-_{rad}), effective charge of all ions(Z^-_{eff}), net power heating(P^-_i)fusion power$(P^-_{fu})$and fusion gain(Q^-), of fuel D-T and $D-{}^3He$ are calculated in terms of temperature variations and their curves are given in the Fig (7) to (15).

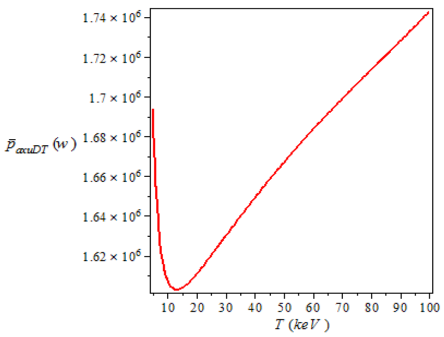

a

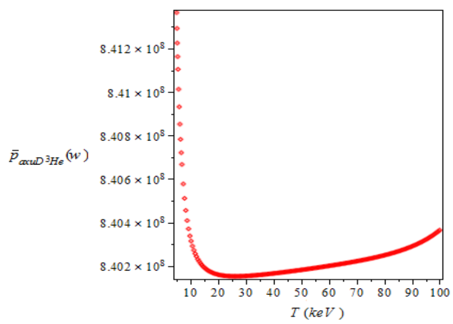

b

Fig7. Auxiliary power of **(a)** D - T and **(b)** $D-{}^3He$at the steady state in the temperature range of 0 to100 (keV)

According to Fig7 can be concluded that auxiliary power of D-T fuel initially is reduced and the temperature about $12KeV$ is minimized then with increasing temperature is increased and at the $100KeV$ temperature is maximized. For $D-{}^{3}He$ this power is maximized at low temperatures then by increasing temperature auxiliary power is reduced and the temperature near $20KeV$ is minimized and then by adding to temperature $100keV$ gradually grows.

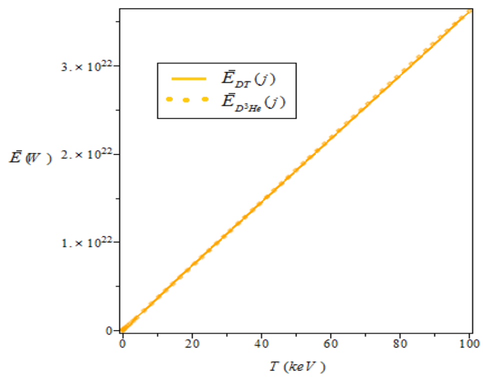

Fig8. Comparison of the total energy of the D-T and $D-{}^{3}He$ fuel in the steady state and temperature range of 0 to100 (keV).

According to the Fig 8 we can find that the total energy of both D-T and $D-{}^{3}He$ fuel with increasing temperature has increased linearly. Because according to equations (20), and (21) the total energy, directly proportional to temperature (T). Since from Fig9 we can see the total densities of $\bar{N}_{DT}$ and $\bar{N}_{D\,{}^{3}He}$ are nearly equal therefore according to the equations (20), and (21), we conclude that the total energy $\bar{E}_{DT}$ and $\bar{E}_{D\,{}^{3}He}$ will be the same.

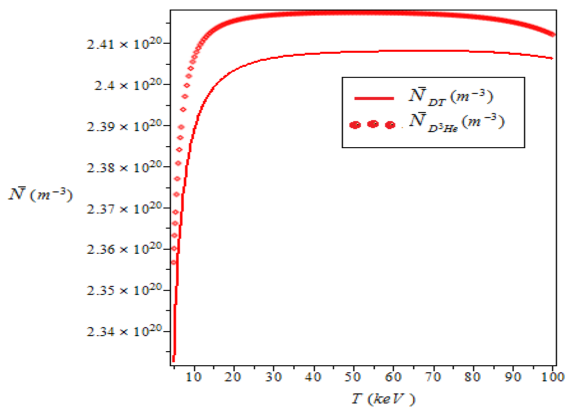

Fig9. Comparison of total density of theD-T and $D-{}^{3}He$fuelin thesteadystate and temperature rangeof 0 to100 (keV).

According to Figure9 can be seen that the total density of the fuel D - T and $D-{}^{3}He$ similar trends with temperature variations and with temperature increasing, their values rapidly increase and then reach to a constant value also from 80 (keV) to 100 kev grows gradually but at all temperatures, the density of $D-{}^{3}He$is greater than D – T. This behavior is due to the kinetic equations governing the system and the shape of equations (24) and (25).

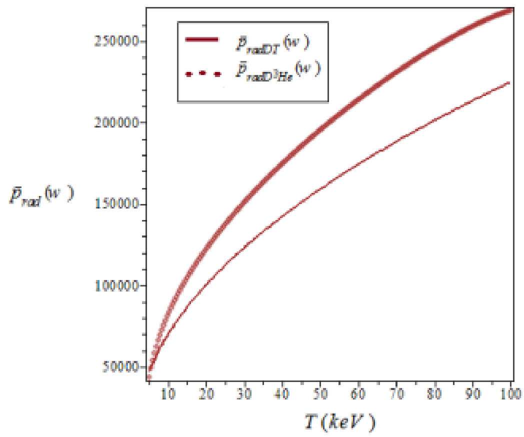

Fig10. Comparison of the radiative loss power for both fuel of D – T and $D-{}^{3}He$ in steady state at temperature interval 0 to100 (keV).

According to Fig 10 can be found that radiative power loss of both fuel D-T and $D-{}^{3}He$ with temperature increasing grows. Because, as the temperature increases, the ions of the plasma, obtain more energy and thus these power increase. Also wecan see that radiative power loss of $D-{}^{3}He$variations at all temperature range is greater than D-T.

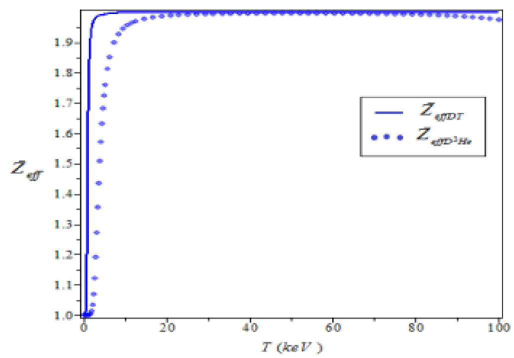

Fig11. Comparison of effective charge of all ions for both D-T and $D-{}^{3}He$fuelin thesteadystate and temperature rangeof 0 to100 (keV).

According to Figure 11 can be found that effective charge of all ions for D-T with increasing of temperature increase and its maximum value is about 1.99 at 5 *kev* then with increasing temperature its value is fixed . For $D-{}^{3}He$ similar performance is occurred except that its maximum value at 24 *kev* is about 1.99 then with increasing temperature till 76 *kev* its value is fixed and after that with growth of temperature its value is reduced very slowly. Also we can see that in the temperature interval 30 to 80 kev Z_{effDT} and $Z_{effD\,{}^{3}He}$ are coincidence.

Also from equation (26) net heating power for both fuel D-T and $D-{}^{3}He$ in the temperature interval 0 to 100 *kev* are plotted (see Fig12).

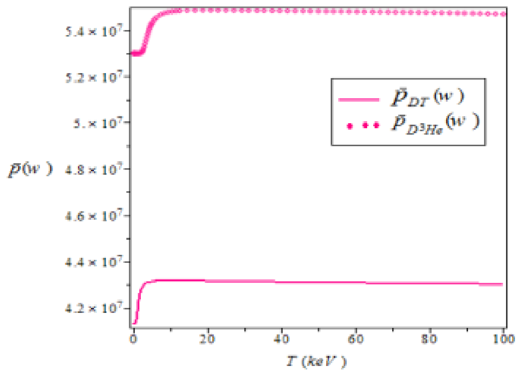

Fig12: Comparison of the net heating power of D-T and $D-{}^3He$ in steady state at temperature interval 0-100 (keV).

AccordingtoFig12 can be found that the value of net heating power of the D – T increases with increasing temperature such that its value changes from $4.12\times 10^7 (W)$to $4.31\times 10^7 (W)$, and then its value slowly and gradually decreases with increasing temperature. But from this figure you can see that the $D-{}^3He$ totalnetheating power is always greater than D -T, in the temperature range 0 to100 (keV).

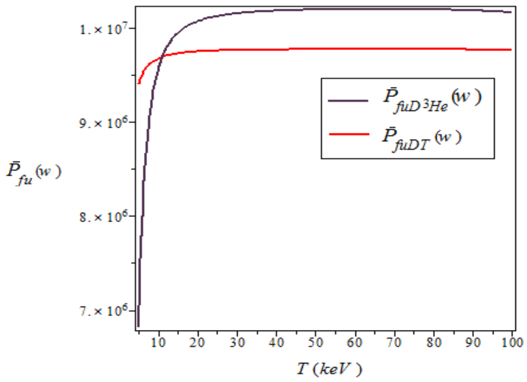

Fig13. Comparison of fusion power for both of D-T and $D-{}^3He$ fuel in the steady state in terms of temperature variations.

According to Fig13, can be found that the fusion power of both fuels D-T and $D-{}^3He$ grows with temperature increasing. Since that the number of fusion reactions is enhanced therefore the fusion power increases. Also, we can see that the fusion power of $D-{}^3He$ fuel is higher than D-T.

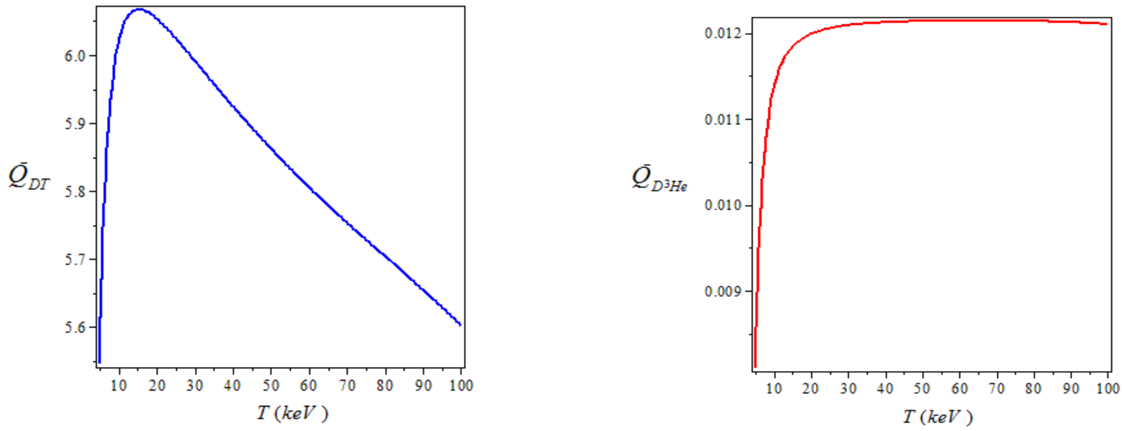

a b

Figure14:fusion gain variations of a)D - T, b) $D-{}^3He$ and fuel in the steady state at the temperature range 0 to100 (keV)and $\boldsymbol{\tau_{EDT} = 3.3\ (s)}$,$\boldsymbol{\tau_{ED\,{}^3He} = 16\ (s)}$

According to figure 14can be found that initially fusion gain of D – T fuel is enhanced with temperature increasing ant its maximum value is about 6, then with temperature growing its value gradually reduced such that at 100kev temperature its Q value reaches 5.

However, $D-{}^3He$ fusion gain with temperature increasing enhances such that at 20 kev temperature reaches to the value 0.012, than with increasing temperature up to 100 kev its value is fixed. In general from this figure we see that fusion gain of D-T is greater than $D-{}^3He$. So in the steady state is not recommended to use the $D-{}^3He$ fuel for the reactor ITER90H-P. For having more realistic information about Q^- for both fuel D-T and $D-{}^3He$ it is better to enter $\tau_E$changes on the fusion gain. (see Fig.15)

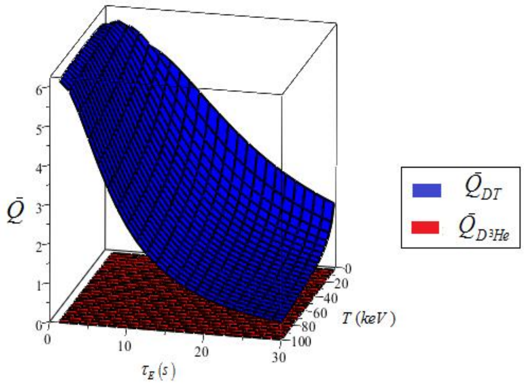

Fig15. Three dimensional variation of fusion gain for D-T and $D-\ ^3He$ fuel, in the steady state at temperature range of 0 to100 (keV) and τ_E range of 0 to30seconds.

Also for having comparison between numerical values forth auxiliary power, fusion power and fusion gain see Table(5).

Table5. Calculated numerical valuesoftheauxiliarypower, fusion power and gain fusion With considering both of fuel D – T and $D-\ ^3He$atsteady statein the temperature range0 to100 keV

T(keV)	$P_{auxD\ ^3He}(W)$ (10^8)	$P_{auxDT}(W)$ (10^6)	$P_{fuDT}(W)$ (10^7)	$P_{fuD\ ^3He}(W)$	Q_{DT}^{-}	$Q_{D\ ^3He}^{-}$
1	8.44	5.404	0.3213	31587.217	0.019	0
10	8.403	1.615	1.004	9.528×10^6	5.992	0.011
20	8.402	1.615	1.004	1.003×10^7	6.01	0.012
30	8.402	1.627	1.004	1.014×10^7	5.973	0.012
40	8.402	1.651	1.004	1.017×10^7	5.916	0.012
50	8.402	1.662	1.004	1.017×10^7	5.841	0.012
60	8.402	1.686	1.004	1.017×10^7	5.785	0.012
70	8.402	1.698	1.004	1.017×10^7	5.729	0.012
80	8.403	1.71	1.004	1.017×10^7	5.691	0.012
90	8.403	1.734	1.004	1.017×10^7	5.635	0.012
100	8.404	1.746	1.004	1.014×10^7	5.616	0.012

Also if in determining of physical quantities such as radiative power loss ,total energy ,net heating power, auxiliary power ,power and fusion gain of both fuel D – T and $D-\ ^3He$we enter the variations of k_d و $k_\alpha$parameters in the range of $0 < k_\alpha < 25$, $0 < k_d < 4$and also by considering fusion power variations for both fuel D – T and $D-\ ^3He$ versus energy confinement time (τ_E) the discussion is wider (see Figs.16 to 20).

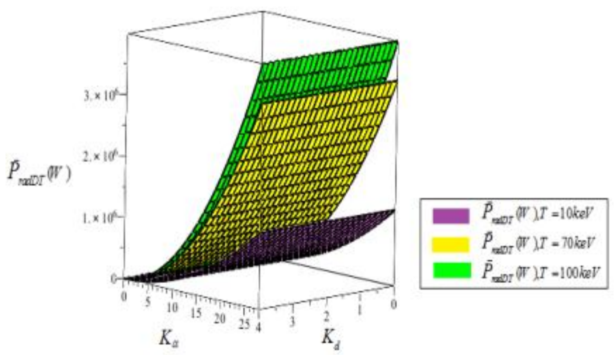

Fig16. Three dimensional comparison of radiative power loss for D – T fuel in steady state at three temperature 10, 70 and 100 kev in terms of $k_\alpha$and $k_d$variations.

With seeing Fig.16 we find that the radiation power loss of D-T fuel increased with increasing temperature and $k_\alpha$and k_d.

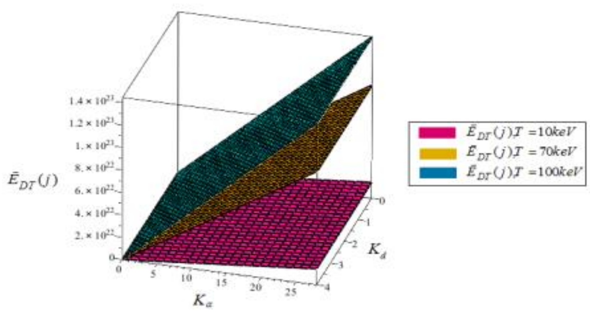

Fig17. Three dimensional comparison of total energy for D – T fuel in steady state at three temperature 10, 70 and 100 kev in terms of $k_\alpha$and $k_d$variations.

From Figure17 can be seen that the total energy of the D-T fuel increases with increasing temperature as k_α and $k_d$change.

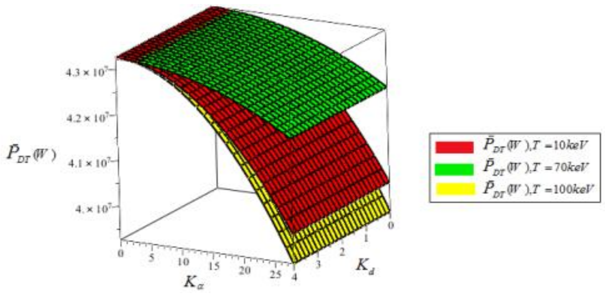

Fig18. Three dimensional comparison net heating power for D-T fuel in steady state at three temperature 10, 70 and 100 *kev* in terms of k_α and k_d variations.

From Figure18can be seen that the net heating power decreases with increasing temperature as k_α and k_d change.

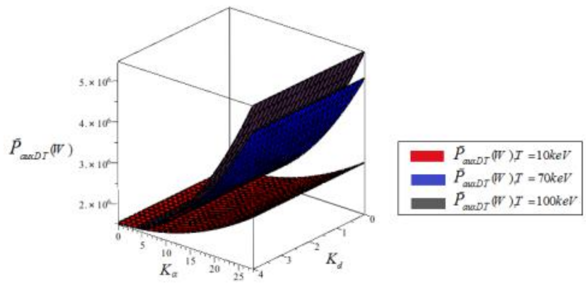

Fig19. Three dimensional comparison auxiliary power for D-T fuel in steady state at three temperature 10, 70 and 100 *kev* in terms of k_α and k_d variations.

We have seen form Fig.19 with increasing temperature eaxillary power (P_{aux}) will rise as k_α and k_d change.

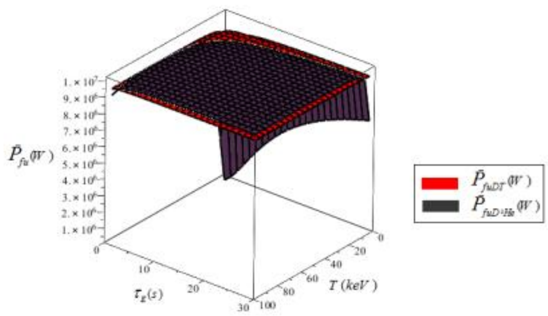

Fig 20. Three dimensional variation of fusion gain for D-T and $D-{}^3He$ fuel in the steady-state at temperature range of 0-100 (*keV*) and energy confinement time range 0-30 seconds

According to figure20 we can say that in all temperature and confinement time variations the fusion power $D-{}^3He$ is greater than D-T.

CONCLUSION AND DISCUSSION

With studying and analyzing ofITER90H-p fusion reactors and solving the non-linear point kinetic equations governing on the two- fuel D-T and $D-{}^3He$ atsteady, dynamical and perturbation states, we find that the main quantities in determining the fusion gain are the densities of alpha particles, deuterium, tritium, helium, neutral fuel, electron , fusion energy and the total energy, and density of total particles, the effective charge of all ions, radiative power loss, auxiliary and fusion power ,respectively. In order to be commercially competitive, a fusion reactor needs to run long periods of time in a stable burning plasma mode at working points which are characterized by a high Q , where Q is the ratio of fusion power to auxiliary power. Active burn control is often required to maintain these near-ignited or ignited conditions (Q = ∞). Although operating points with these characteristics that are inherently stable exist for most confinement scaling, they are found in a region of high temperature and low density. Our studies show that in the steady-state above quantities are only a function of temperature and each has its own specific variations and also at the temperature70 (keV) these quantities produce the maximum fusion gain for both of fuels D-T and $D-{}^3He$ such that their values are equal to 6.01 for D - T fuel-andthe0.012 for $D-{}^3He$, respectively. Fusion using $D-{}^3He$ fuel requires significant physics development particularly of plasma confinement in high performance alternate fusion concepts. Countering that cost, engineering development cost should be much less for $D-{}^3He$ than D-T, because $D-{}^3He$ greatly ameliorates the daunting obstacles caused by abundant neutrons and the necessity of tritium breeding. A $D-{}^3He$ fusion fueled fusion reactor would also possess substantial safety and environmental advantages over D-T. Currently recommended for reactor ITER90H-p is used D-T fuel and still need more research to be done on the fuel $D-{}^3He$.

REFERENCES

Bosch, H.-S., & Hale, G. (1992). Improved formulas for fusion cross-sections and thermal reactivities. *Nuclear Fusion, 32*(4), 611.

Eremin, A., & Shishkin, A. (2008). Fusion D+ T and D+ D products dynamics for the different fueling scenarios in toroidal magnetic reactors.

Hively, L. (1977). Special topic convenient computational forms for maxwellian reactivities. *Nucl. Fusion, 17*(4), 873.

Kadomtsev, B. (1992). Tokamak Plasma: A Complex Physical System IOP: Bristol.

Pinna, T., & Rizzello, C. (2002). Safety assessment for ITER-FEAT tritium systems. *Fusion engineering and design, 63*, 181-186.

Schuster, E., Krstic, M., & Tynan, G. (2003). Burn control in fusion reactors via nonlinear stabilization techniques. *Fusion science and technology, 43*, 18-37.

Spitzer Jr, L. (1965). Physics of Fully Ionized Gases (Interscience, New York, 1962). *Chap, 5*, 143.

Spitzer, L. (2013). *Physics of fully ionized gases*: Courier Dover Publications.

Trintchouk, F., Yamada, M., Ji, H., Kulsrud, R., & Carter, T. (2003). Measurement of the transverse Spitzer resistivity during collisional magnetic reconnection. *Physics of Plasmas (1994-present), 10*(1), 319-322.

Uckan, N. A. (1993). *Confinement capability of ITER-EDA design.* Paper presented at the Fusion Engineering, 1993., 15th IEEE/NPSS Symposium on.

Uckan, N. A., Hogan, J., Houlberg, W., Galambos, J., Perkins, L., Haney, S., . . . Kaye, S. (1994). ITER design: physics basis for size, confinement capability power levels and burn control: Oak Ridge National Lab., TN (United States). Funding organisation: USDOE, Washington, DC (United States).

Wesson, J. (2011). *Tokamaks* (Vol. 149): Oxford University Press.